

MIDDLE-EAR FINITE-ELEMENT MODELLING WITH REALISTIC GEOMETRY AND A *PRIORI* MATERIAL-PROPERTY ESTIMATES

Chadia S. Mikhael¹, W. Robert J. Funnell^{1, 2}, and Manohar Bance³

¹Department of BioMedical Engineering ²Department of Otolaryngology
McGill University, Montréal, QC

³Depts. Surgery and Anatomy & Neurobiology, Dalhousie University, Halifax, NS

ABSTRACT

Finite-element models of the middle ear have generally included oversimplified geometries, and many of their material properties have often been estimated by curve fitting to averaged experimental vibration measurements from multiple ears. As a result, the parameter values may not be physiologically reasonable. Our study aims to construct a valid middle-ear finite-element model without such curve fitting by (1) creating realistic geometries, and (2) using *a priori* estimates for the material properties.

We began by scanning a human temporal bone using x-ray micro-computed tomography. Details of middle-ear structures were then segmented, both manually and semi-automatically. The substructures were assigned appropriate material properties – including thickness, Young's modulus, and Poisson's ratio – based on a detailed literature review, and a finite-element model was generated.

The static behaviour of this model was compared with low-frequency measurements performed on the same temporal bone using laser Doppler vibrometry. Preliminary results show good model accuracy with regard to footplate and eardrum displacements, and agreement within a factor of about two for umbo displacement. A sensitivity test was done to identify those material properties which have strong effects on the model behaviour.

INTRODUCTION

The finite-element (FE) method is a numerical method that has been applied in many fields to simulate complex systems. The first attempt to model middle-ear mechanics via the FE method was in 1978¹. Since then, numerous models have followed^{e.g., 2-5}. Such models have proven useful for understanding middle-ear mechanics, for analysing middle-ear prostheses and for teaching purposes.

The human ear consists of three compartments: the outer, middle and inner ears. The outer ear captures sound waves traveling in the air and funnels them through the external auditory canal towards the middle ear. The middle ear transmits mechanical energy across the ossicular chain to the inner ear, where it is transformed into electrical signals and transmitted to the brain for interpretation. The middle ear consists of an air cavity containing three small bones, two muscles and several joints and ligaments.

Most middle-ear models are generated with simple ligament geometries, followed by iterative alterations in structure material properties until the model behaviour matches averaged experimental vibration measurements from multiple middle ears. As a result, the

chosen parameter values may not be physiologically reasonable, and the models may not be valid even though they appear to fit averaged data. When structure modifications are later required to represent different middle-ear scenarios, additional curve fitting with new material properties becomes necessary.

The purpose of this study is to try to achieve an accurate FE model of the middle ear without using fitting for the material-property parameters. This is approached by emphasising realistic substructure geometry from a specific ear and using *a priori* material-property estimates. The model's response will then be compared with displacements measured in the same ear by means of laser Doppler vibrometry (LDV).

MATERIALS AND METHODS

Geometry

To obtain an accurate geometry for the middle-ear structures, an x-ray micro-computed tomography (μ CT) scan of the middle ear was performed (using a Skyscan 1072 scanner), yielding 1024 sections, each with a thickness and pixel size of 19 μ m. To speed processing, the dataset was downsampled by half, reducing the number of slices to 512 and increasing their thickness and pixel size to 38 μ m.

Next, we segmented the middle-ear structures with a home-grown programme, *Fie*⁶ (*Fabrication d'imagerie extraordinaire*). Manual segmentation was used to outline thin open structures, such as the tympanic membrane (TM), as well as the general shapes of the other structures of interest. This was followed by semi-automatic segmentation using a *snake* algorithm^{7,8} in combination with two-level thresholding.

Figure 1 shows the components of our model. These include the TM (pars flaccida and pars tensa = PF and PT in the figure), ossicles (malleus, incus and stapes), joints (incudomalleal and incudostapedial joints = IMJ and ISJ), and ligaments (anterior malleal ligament = AML, superior malleal ligament = SML, posterior incudal ligament = PIL, stapes annular ligament = SAL, and the ligament joining the TM to the manubrium = TM-MAN LIG).

We generated a mesh of triangular thin-shell elements using a home-grown programme, *Tr3*. This geometrically reasonable mesh comprises a total of 1871 nodes and 3831 elements. The mesh was passed to a FE package, *SAP IV*⁹, to simulate the model's behaviour in response to a static pressure of 1 Pa applied to the lateral surface of the TM.

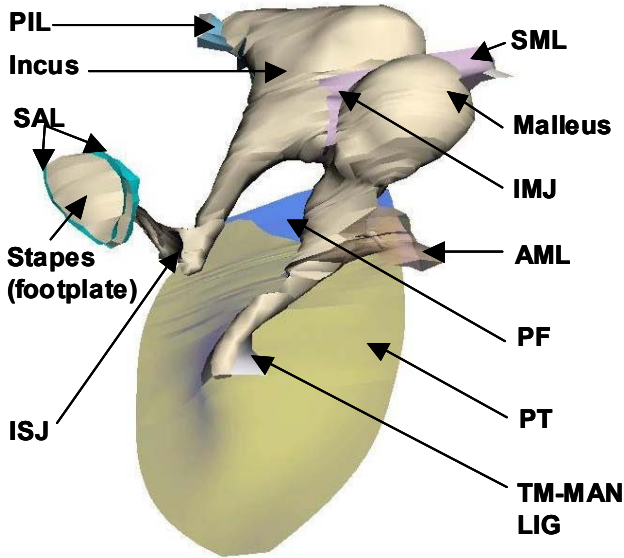


Figure 1. 3-D model of a human middle ear

We also tested the effects of higher mesh resolutions on an earlier, slightly different version of this model. Increasing the number of elements per diameter by 46% changed the maximum TM and stapes displacements by only 10% and 6%, respectively. Doubling the number of slices used in the model changed the maximum TM and stapes displacements by 11% and 38%, respectively.

Material Properties

We assumed the model to be isotropic and linearly elastic with uniform thickness throughout each of its structures. Also, since our study was limited to low frequencies, we were able to neglect inertial and damping effects, including those of the cochlea.

The Young's moduli and thicknesses of our model's structures are summarized in Table 1. The Young's moduli were deduced from a thorough literature review on isolated or semi-isolated studies of analogous structures. The thicknesses were set to approximately one-third of the structures' total thicknesses, as seen in the μ CT slices. Given the small effect that Poisson's ratio has on the response of the middle ear¹⁰, all structures were assigned the same value, 0.3.

Boundary Conditions

The tympanic membrane – both PF and PT – was fixed around its entire circumference, representing its attachment to the walls of the external auditory canal via the fibrocartilaginous ring; the ring itself was not explicitly included in our model. In addition, the AML, SML, and both bundles of the PIL were clamped to the walls of the tympanic cavity, and the SAL was clamped to the oval window.

	Young's Modulus (MPa)	Average thickness (μ m)
TM:		
<i>Pars flaccida</i>	20 [11]	200 [16]
<i>Pars tensa</i>	40 [12]	75 [12]
Ossicles:		
<i>Malleus & incus</i>	200 [2]	90
<i>Stapes</i>	200 [2]	29
Ligaments:		
<i>SML, AML</i>	20 [13]	63
<i>IM joint</i>	200	50
<i>PIL</i>	20 [11]	47
<i>IS joint</i>	50 [14]	21
<i>Stapes ann. lig</i>	0.01 [15]	20
TM-MAN LIG:		
-mid-region	2	35
-ligament ends	20	

Table 1. Material properties assigned to the ME structures for creating a FE model.

LDV Measurements

The frequency response of the same middle ear was measured using LDV at Dalhousie University. The experimental stimuli were frequency sweeps over the range of 0.25 to 8 kHz, at 90 dB SPL, and displacements were recorded at 3 different places on each of the TM and stapes footplate. The low-frequency response, from 250 to 300 Hz, was then averaged (due to the large amount of noise observed at low frequencies) and compared with the response of our FE model for an assessment of the latter's accuracy. We compared maximum TM displacement, maximum footplate displacement and umbo displacement, as measured by LDV, with the corresponding displacements of the model.

Sensitivity Test

To better identify the most influential model parameters, we tested the model's sensitivity to the Young's modulus (Y) of seven structures (Y_{PT} , Y_{PF} , Y_{AML} , Y_{SML} , Y_{PIL} , Y_{ISJ} , Y_{SAL}) and the thicknesses (T) of two structures (T_{PF} and T_{PT}) one at a time, at $\frac{1}{4}$, $\frac{1}{2}$, $1\frac{1}{2}$, and 2 times their nominal values; a wider range was also studied for Y_{SAL} and Y_{ISJ} .

RESULTS

Finite-Element Model vs. LDV Data

A comparison between the FE model's response and the average low-frequency response of the same ear, measured by LDV, showed reasonable similarity. As seen in Table 2, our model estimated TM and stapes footplate displacements to within approximately 10% and 16%, respectively. The umbo displacement agreed within a factor of about 2.

	FE model response (in nm)	LDV measurements (in nm)
TM	109.1	99.4
umbo	84.1	40.6
footplate	17.2	20.5

Table 2. Low-frequency FE model behaviour versus LDV measurements on the same middle ear.

Sensitivity Analysis

The effects of 9 parameters on the FE model's behaviour are summarized in Figures 2 and 3. TM displacement (Figure 2) proved to be most sensitive to pars-tensa thickness, followed by pars-tensa Young's modulus; the remaining 7 parameters had relatively little effect. Footplate displacement (Figure 3) was also sensitive to pars-tensa thickness and Young's modulus, and in addition was quite sensitive to pars-flaccida thickness; the other 6 parameters had significantly smaller effects.

For the ranges of Young's moduli included in Figure 3, the effects of incudostapedial-joint stiffness (Y_{ISJ}) and stapes annular-ligament stiffness (Y_{SAL}) were very small, which is rather surprising. We decided, therefore, to explore the effects of those 2 parameters over a wider range. For Y_{ISJ} , we noted steadily increasing footplate displacement from 1 kPa until 1.5 MPa, after which it dropped slightly (Figure 4). This could be explained by a loss of energy in the joint when it is too flexible, and by a need for excessive sideways footplate displacement when the joint is too stiff. Y_{SAL} , on the other hand, showed a strong influence on footplate displacement for stiffnesses beyond about 20 kPa (Figure 5).

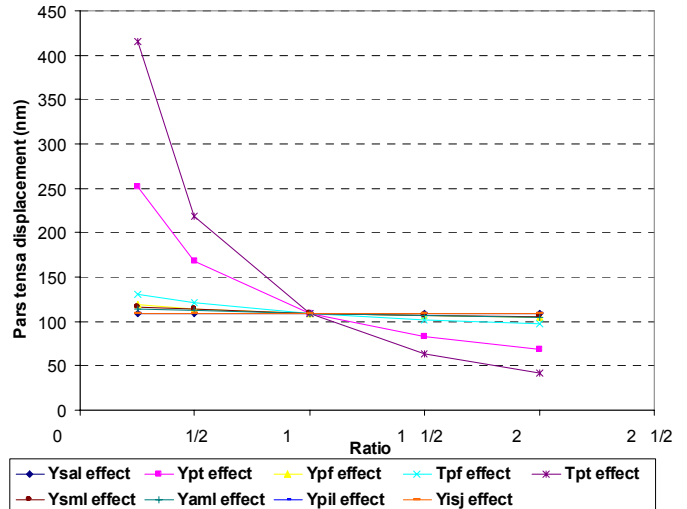


Figure 2. Parameter effects on TM displacement.

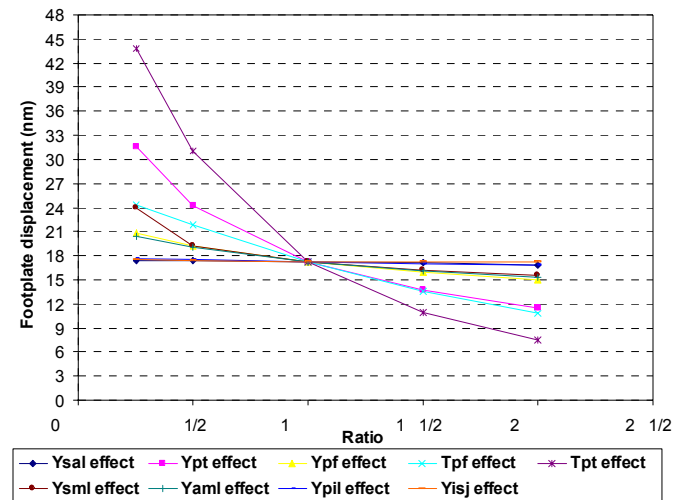


Figure 3. Parameter effects on footplate displacement.

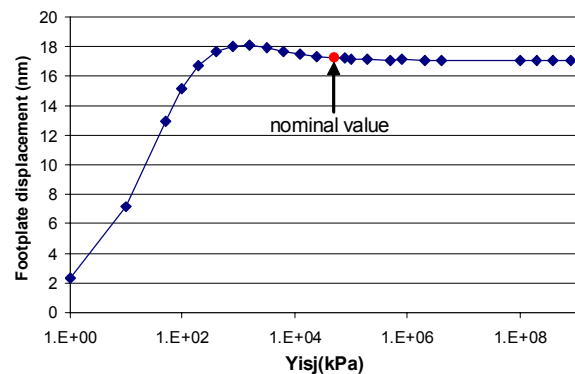


Figure 4. The sensitivity of footplate displacement with respect to Y_{ISJ} .

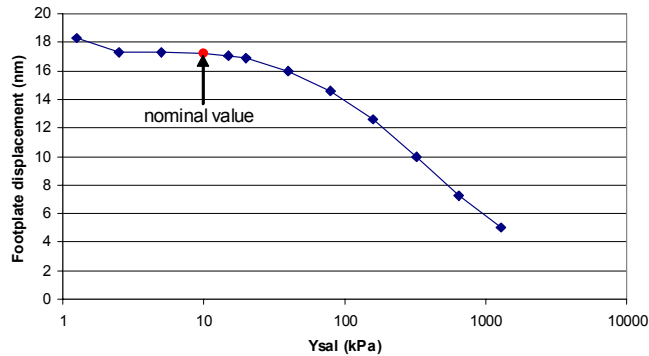


Figure 5. Footplate displacement is equally sensitive to Y_{SAL} between 2.5 and 10 kPa and is less sensitive at higher stiffnesses.

CONCLUSIONS

We generated a FE model of the middle ear. It includes the TM, the ossicles, four suspensory ligaments, and the incudomalleal and incudostapedial joints. We accurately derived the geometry of the model from μ CT slices, and assigned material properties based on *a priori* estimates deduced from a detailed literature review.

This model proved to replicate the experimentally measured low-frequency behaviour of the individual middle ear which it represented with good accuracy for both TM and stapes displacements and within a factor of about 2 for manubrium displacements.

This study seems to support the feasibility of generating accurate FE models for individual ears based on detailed geometry and *a priori* material-property estimates, without the need for curve fitting to estimate the material-property parameters. This model is preliminary, however, and improvements need to be made. Implementing solid elements will be essential to correctly represent the soft tissues of the ear. Taguchi analysis may be helpful in providing an insight into individual parameter effects as well as potentially significant interactions between them¹⁷. Furthermore, dynamic analysis will be necessary to investigate the model's response across the range of hearing frequencies.

Once such a realistic and reliable model is available, it can be employed to study a range of middle-ear defects and injuries, diagnostic tools and corrective techniques.

ACKNOWLEDGEMENTS

This work was supported by the Canadian Institutes of Health Research and the Natural Sciences and Engineering Research Council of Canada.

REFERENCES

1. Funnell WRJ and Laszlo CA, "Modeling of the cat eardrum as a thin shell using the finite element method", J. Acoust. Soc. Am. 63, 1461-1467, 1978.
2. Funnell WRJ, Khanna SM, Decraemer WF, "On the degree of rigidity of the manubrium in a finite-element model of the cat eardrum", J. Acoust. Soc. Am. 91, 4, 2082-2090, 1992.
3. Beer HJ, Bornitz M, Drescher J, Schmidt R, Hardtke HJ, Hofmann G, Vogel U, Zahnert T, Huttenbrink K-B, "Finite element modelling of the human eardrum and applications", Proc. Of the Int. Workshop on Middle Ear Mechanics in Research and Otosurgery, Dresden, Germany, September 19-22, 1996/ ed. by Huttenbrink K-B. Dresden University of Technology, 40-47, 1997.
4. Sun Q, Gan RZ, Chang K-H, Dormer KJ, "Computer-integrated finite element modeling of human middle ear", Biomechan. Model. Mechanobiol. 1, 109-122, 2002.
5. Koike T, Wada H, Kobayashi T, "Modeling of the human middle ear using the finite-element method", J. Acoust. Soc. Am., 111, 1306-1317, 2002.
6. <http://audilab.bmed.mcgill.ca/~funnell/AudiLab/sw/fe.html>.
7. Kass M, Witkin A, Terzopoulos D, "Snakes: active contour models", Internat. J. Comp. Vision, 3, 321-331, 1986.
8. Hatamzadeh-Tabrizi J and Funnell WRJ, "Comparison of gradient, gradient vector flow and pressure force for image segmentation using active contours", Proc. 27th Ann. Conf. Can. Med. Biol. Eng. Soc., 2002.
9. Bathe K-J, Wilson EL, Peterson FE, "SAP IV. A Structural Analysis Program for Static and Dynamic Response of Linear Systems", Report No. EERC 73-11 (University of California, Berkeley), 1974.
10. Funnell WRJ, "A Theoretical Study of Eardrum Vibrations Using the Finite-Element Method", Ph.D.Thesis, McGill University, Montréal, 1975.
11. Funnell WRJ, "Finite-element modeling of the cat middle ear with elastically suspended malleus and incus", 19th Midwinter Res. Mtg., Assoc. Res. Otolaryngol., St. Petersburg Beach, 1996.
12. Kirikae I, "The Structure and Function of the Middle Ear", The University of Tokyo Press, 1960.
13. Funnell WRJ, Decraemer WFS, von Unge M, Dirckx JJJ, "Finite-element modelling of the gerbil eardrum and middle ear", 23rd Midwinter Res. Mtg., Assoc. Res. Otolaryngol., St. Petersburg Beach, 2000.
14. Siah TS, "Finite Element Modeling of the Mechanics of the Coupling Between the Incus and Stapes in the Middle Ear", M. Eng Thesis, McGill University, Montréal, 2002.
15. Lynch TJ, Nedzelnitsky V, Peake WT, "Input impedance of the cochlea in cat", J. Acoust. Soc. Am., 72, 108-130, 1982.
16. Ladak HM and Funnell WRJ, "On the effects of geometric nonlinearities in a finite-element model of the cat eardrum", Proc. IEEE EMBS 17th Annual Conference & 21st Can. Med. & Biol. Eng. Conf., Montréal, 1439-1440, 1995.
17. Qi L, Mikhael CS, Funnell WRJ, "Application of the Taguchi method to middle-ear finite-element modelling", Proc. 28th Ann. Conf. Can. Med. Biol. Eng. Soc., 2004.